GEOPHYSICS, VOL. 62, NO. 3 (MAY-JUNE 1997); P. 786–796, 10 FIGS.

Use of ground-penetrating radar for 3-D sedimentological characterization of clastic reservoir analogs

George A. McMechan*, Gerard C. Gaynor‡, and Robert B. Szerbiak*

ABSTRACT

Clastic reservoir analogs based on 2-D outcrop studies provide valuable definitions of geometric and petrophysical heterogeneities at interwell scales. Integration of 3-D ground-penetrating radar (GPR) surveys with sedimentological and stratigraphic data provides information on the internal heterogeneities of sedimentary sequences at scales that allow dissection of the 3-D anatomy of clastic depositional systems. Two 3-D GPR data volumes were acquired in the Ferron sandstone of east-central Utah. The data show prominent lenticular features, a variety of lithologies, and structural elements such as channels and shale drapes that match well with those seen at the same stratigraphic levels in adjacent cliff faces.

INTRODUCTION

Knowledge of the distributions of porosity and permeability in an oil or gas reservoir is important because they control the volume and movement of reservoir fluids. Accurate models are needed for cost-effective reservoir simulation and for well placement strategies for maximizing recovery of hydrocarbons. However, direct sampling of the reservoir is restricted to a well bore and the adjacent rock volume, so spatial variations in interwell reservoir properties can only be estimated. Outcrop studies of reservoir analogs are one way to observe 2-D geometries of the clastic depositional systems that control porosity and permeability in similar units in the subsurface (Tyler et al., 1992; Fisher et al., 1993a,b). Generalization to the third spatial dimension is necessary. For example, Henriquez et al. (1990) demonstrate the importance of the interconnectedness and orientation of fluvial channels in simulation design. At present, these factors can only be estimated from empirical formulas (Allen, 1979). New technologies for 3-D reservoir characterization are necessary to improve accuracy and reliability in reservoir modeling.

Studies of outcrops of reservoir analogs can benefit significantly by integration of sedimentologic and stratigraphic data sets with 3-D ground-penetrating radar (GPR) images. The effectiveness of GPR for characterizing reservoir geometry and heterogeneity through studies of shallow analogs has been demonstrated in 2-D profiles (Baker, 1991; Pratt and Miall, 1993; Gawthorpe et al., 1993; Meyers et al., 1994), but the full benefit can best be realized by doing 3-D GPR surveys. In this project, we acquired pseudo 3-D GPR data on a grid of closely spaced 2-D lines. Unlike conventional high-resolution seismic data whose resolution of >10 m can be utilized only for locating reservoir rocks, the subdecimeter resolution of GPR can be employed for dissecting the anatomy of individual reservoirs (Miall, 1988; Jordan and Pryor, 1992).

In this paper, we report the results of a successful 3-D pilot study performed in east-central Utah in the fall of 1994. This site has a large existing sedimentologic and stratigraphic data base (Fisher et al., 1993a,b), and so is ideal for evaluation of the GPR technique for analysis of reservoir analogs.

RESERVOIR DESCRIPTION USING ANALOGS

Precise 3-D models, which describe specific geometries and relationships of reservoir units and barriers or baffles, are needed in numerical simulations for forecasting of field performance. These models are also required for field development, including well locations, well-pattern design, and surface facility specifications. In general, the information necessary to construct such models is not available from well data, particularly in the early phases of field delineation and development. Even in intensively drilled fields, the spacing of well logs is large compared to the scale of the spatial variation in petrophysical properties in a reservoir. Drill-stem and wireline testing of reservoir pressure trends can provide estimates of well-to-well communication or reservoir interconnectedness, but interpretation of these results is often nonunique.

Manuscript received by the Editor July 18, 1995; revised manuscript received July 3, 1996.
*Center for Lithospheric Studies, The University of Texas at Dallas, P.O. Box 830688, Richardson, Texas 75083-0688.
‡Formerly Reservoir Geosystems, Inc., 5616 Milton Street, Suite 312, Dallas, Texas 75206; presently ARCO Exploration and Production, 2300 West Plano Parkway, Plano, Texas 75075.

In the absence of geologic and sedimentological models, it is common practice to linearly interpolate reservoir attributes between wells (Armitage and Norris, 1991). However, even preliminary outcrop studies have shown that linear interpolation is invalid. Polasek and Hutchinson (1967) and Ravenne et al. (1987) show that outcrop measurements are valuable in evaluating, and building models for, heterogeneous reservoirs.

Clastic reservoir analogs have been used extensively to assist in characterization of reservoir heterogeneities (Stalkup and Ebanks, 1986), particularly to provide model input for numerical simulations (Tomutsa et al., 1991; Weber and van Geuns, 1989). In a well-documented example, Mayer and Chapin (1991) show that outcrop studies of analogous reservoir systems can be used to define geometric and petrophysical characteristics at interwell scales in the subsurface.

Reservoir simulation involves the modeling of fluid behavior in porous rocks by mathematical equations that approximate the physical processes of fluid flow. A field can be developed only once, whereas simulation under varying producing schemes can be performed numerous times. The best 3-D simulations incorporate detailed geologic models (Weber and van Geuns, 1989). Few outcrop studies are specifically designed to provide input to reservoir simulations (Gundesö and Egeland, 1990; Haldorsen and Damsleth, 1990; Fält et al., 1991; Tyler et al., 1992; Fisher et al., 1993a,b). The integration of GPR and outcrop data may overcome many of the limitations that are associated with the lack of 3-D information in current reservoir characterization studies of outcrop analogs.

RESERVOIR ANALOG TEST AREA

A test site, about 5 km east of Emery in east-central Utah (Figure 1), was chosen for the project. The site is a mesa top with cliff faces exposed by creek erosion on two sides. The mesa has a structural dip of 6 degrees to the northwest. The Ferron sandstone at this site is a deltaic sequence of Cretaceous age, which, because of its excellent exposure, has been studied extensively for stratigraphy and for the relationship of bedforms to permeability distributions (Fisher et al., 1993a,b).

The general stratigraphy of the Ferron sandstone in the outcrop area is well known (Hale, 1972; Cotter, 1975; Ryer, 1981a,b, 1983; Fisher et al., 1992; 1993). The Ferron is composed of seven distinct pulses of deltaic sedimentation termed Genetic Sequences (GS 1-7) by Ryer (1981a). The lowermost sequences (GS 1-3) are interpreted to be progradational; the uppermost (GS 6-7), retrogradational; and GS 4-5, vertically stacked.

The entire outcrop is a fluvial to proximal marine sand member of the Mancos shale. The sequence (Figure 2) consists of shoreface sands (labeled A) that are overlain by a complex series of distributary channel and channel abandonment sands (labeled B). The sandstone dominated bedforms are defined by low-permeability drapes of siltstone and shale. It is these material contrasts that enable GPR to image both individual bedding structures and larger depositional units. Minor heterolithic coal-bearing sequences are also present; readily correlated coal-bearing beds are present near the top of both the GS 5 and GS 6 (Figure 3).

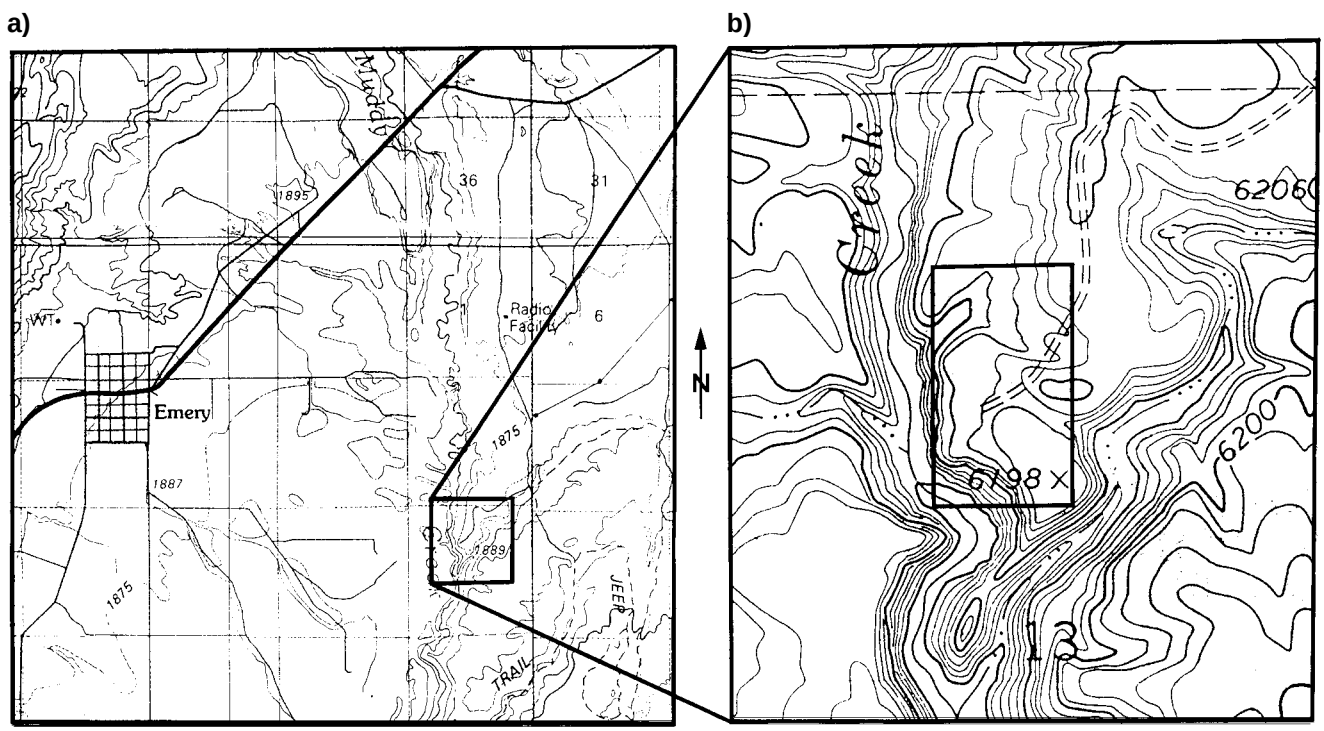

FIG. 1. Location maps for the GPR survey site. It is in section 13 of R6E, T22S. (a) shows the relation to the town of Emery and the road used to access the site. (b) is a more detailed view of the area outlined in (a). For scale, in (a), the grid is 1 mile × 1 mile section lines. In (b), the contour interval is 20 ft. The box in (b) is redrawn in Figure 4 to show the location and orientation of the two 3-D surveys. (a) is from the 1980 USGS 1:100,000 scale metric topographic map of the Salina, Utah 30 × 60 minute quadrangle; (b) is from the 1978 USGS 1:24,000 scale 7.5 minute series topographic map of the Emery East quadrangle.

Outcrop studies indicate that fluvial to distributary channel, delta front, and shoreface sandstone reservoir analogs are present in the study area (Figures 2 and 3). Reservoir baffles and barriers of various scales present in these Ferron sandstone outcrops include shale drapes on bedforms, shales defining lateral accretion surfaces, discontinuous randomly distributed shales, and carbonate concretions.

A conjugate set of near-vertical fractures with diagentically altered (oxidized) surfaces is seen on the exposed bedding planes at the northern-most of our surveys. Large-scale bedforms of major fluvial systems can be seen on the cliff faces; small-scale sigmoidal features and cross-bedded laminae are evident (Figures 2 and 3).

The general area has been extensively studied in both surface outcrop and the subsurface, and has been used by major oil companies and teaching groups for training exploration and production geologists, and for identifying subsurface reservoir analogs. As a result, much of the geologic data are now in the public domain (Katich, 1954; Doelling, 1972; Cleavinger, 1974; Cotter, 1975; Uresk, 1979; Ryer et al., 1980; Ryer, 1981a,b; Thompson, 1985; Ryer and McPhillips, 1983; Lowry, 1990).

GPR SURVEYS

Background

GPR is an electromagnetic method that, in many ways, is similar to seismic reflection. A transmitting antenna radiates an electric pulse into the ground that, under ideal conditions, behaves kinematically similar to an acoustic wave. The pulse is transmitted, reflected, and diffracted by features that correspond to changes in the electrical properties of the earth. The waves that are reflected and diffracted back toward the earth's surface may be detected by a receiving antenna, amplified, digitized, displayed, and stored for further analysis. Good descriptions of the GPR technique and equipment are presented by Daniels et al. (1988), Davis and Annan (1989), Wright et al. (1989), and Boucher and Galinovsky (1989).

The GPR propagation velocity increases as the relative dielectric permittivity decreases, and attenuation increases as electrical conductivity increases. Propagation paths can be predicted from the velocity distribution by ray tracing using Snell's law; reflection and transmission coefficients can be calculated from the contrasts in electrical impedance (e.g., Davis and Annan, 1989).

The transmitter and receiver units are usually separate, so the survey design is flexible. A GPR survey usually proceeds by recording a trace at each of a large number of survey points along a line (or over a grid) with a fixed transmitter-receiver offset. As for seismic data, these 2-D sections may be plotted directly, or combined and plotted as volumes. The main differences are that the scale of a GPR survey is about three orders of magnitude smaller than that of a reflection seismic survey, and the resolution is correspondingly high. GPR frequencies are usually between 10 and 1000 MHz, the time sample increment is usually about 1 ns, the propagation velocities are one-quarter to one-half that of light in a vacuum, and the maximum depth of penetration is usually 10–20 m, depending primarily on the electrical conductivity of the subsurface materials. Reflections and diffractions in a GPR section are a consequence of changes in electrical properties; the latter can usually be correlated with visible sedimentary structures and sequence boundaries.

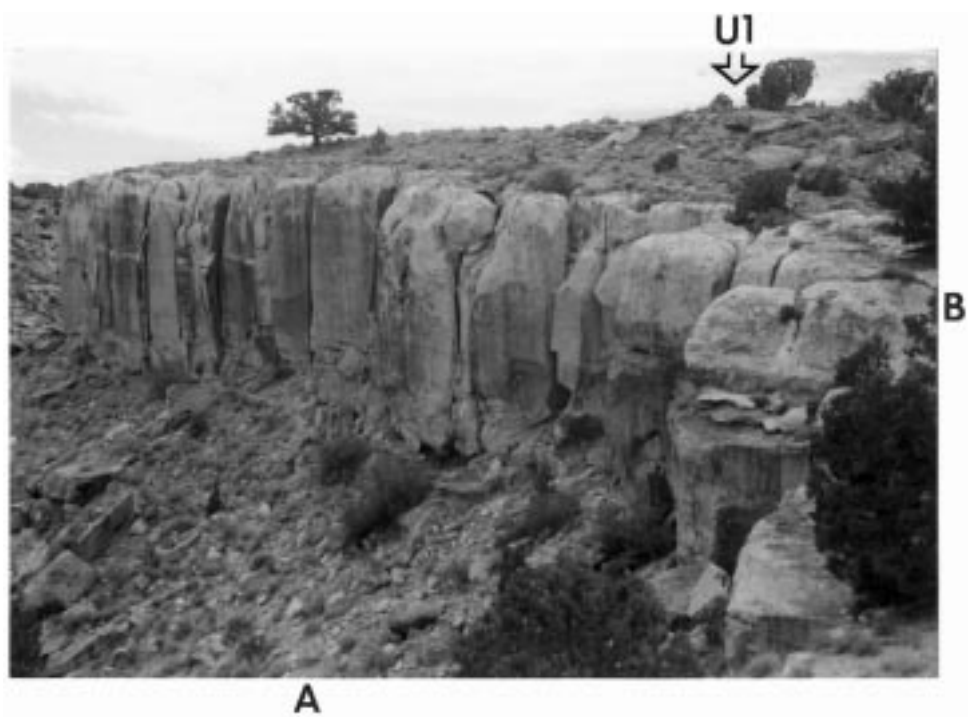

FIG. 2. Photograph of the location of measured section in Figure 3. The camera is pointing toward the northwest. The base of the section is hidden from view. The top of the section corresponds to the eastern corner of GPR survey U1 (arrow). The highest elevation is rocks of GS 7; most of the outcrop is GS 6 (refer to Figure 3). A and B are described in the text.

By exploiting the kinematic similarities between GPR and seismic data, it is possible to borrow advanced data processing and imaging techniques from seismology (Fisher et al., 1992a,b). This analogy no longer holds when accurate amplitude analysis is required; this needs explicit consideration of electromagnetic wave propagation and boundary conditions.

Survey procedures

The GPR data acquired in our study included common-midpoint (CMP) gathers and 3-D volumes. The CMP data were collected at 50, 100, and 200 MHz to determine optimal data acquisition parameters, and for velocity estimation. The 3-D data volumes each consist of a suite of common-offset traces recorded at each point of a closely spaced areal grid; physically, the acquisition was a series of parallel 2-D lines that were then combined to form the volume. Two 3-D surveys were performed; their geometries, orientations, and relative positions are shown in Figure 4. The first (U1) was near the topographic high at the southeast edge of the mesa; the second (U3) was about 230 m northwest of U1, in an erosional scour in the mesa top near the bank of Muddy Creek (Figure 1b). The 2-D lines within the 3-D grids are oriented to be approximately parallel to the structural dip (northwest-southeast).

For efficiency, all odd numbered lines in both 3-D surveys were run in one direction (northwest to southeast) and the even numbered lines were run in the opposite direction. During preprocessing all the even numbered lines were reversed, so all the GPR survey line plots below are presented with distance increasing along the horizontal axis from northwest to southeast.

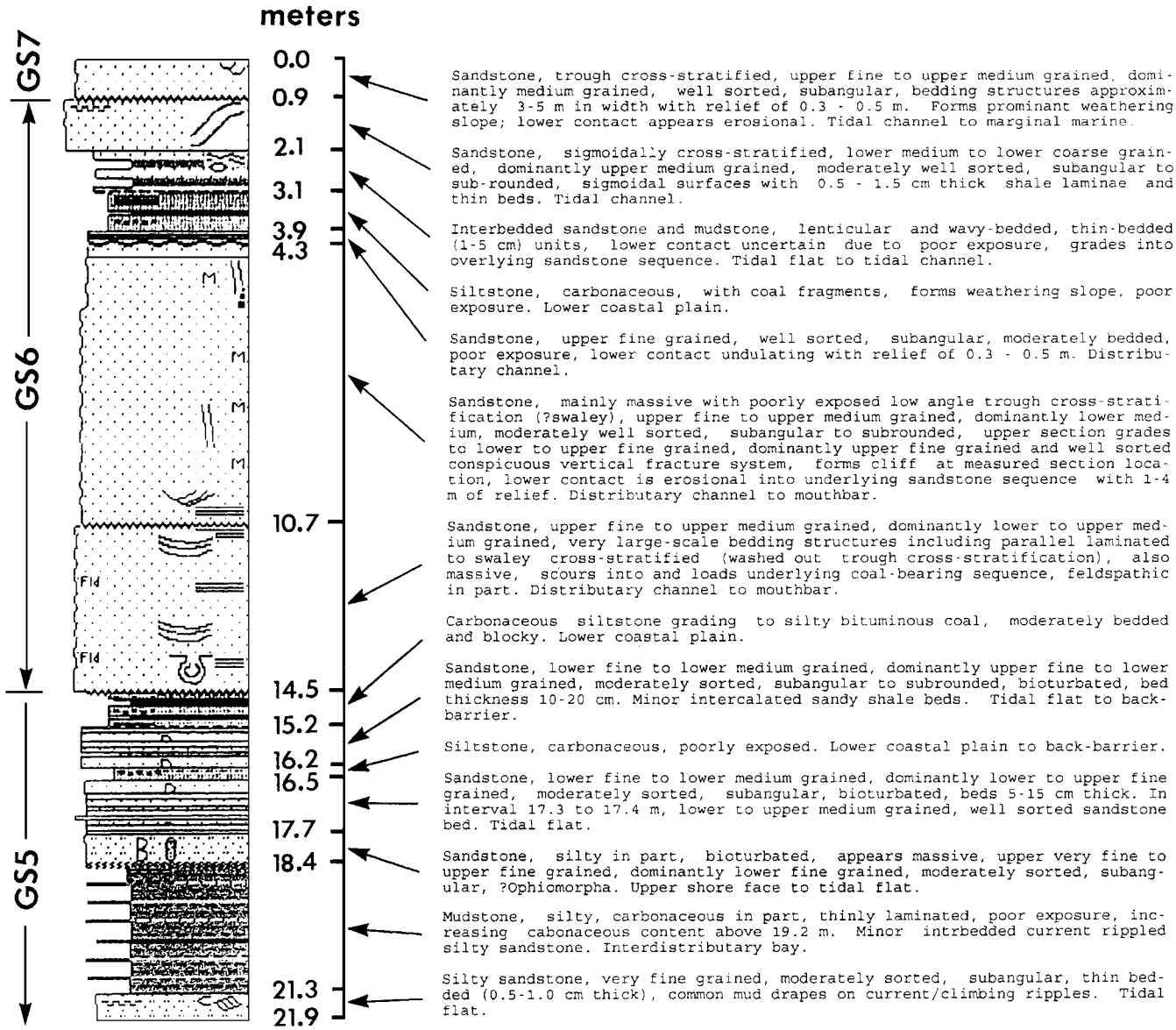

FIG. 3. Measured section through part of the Ferron. Vertical positions are referenced to the point of local maximum elevation, which is near the eastern corner of survey U1 (compare Figures 1 and 4). GS 5, GS 6, and GS 7 are the uppermost genetic sequences of the Ferron (Ryer, 1981a). This section was measured by the second author as part of this project.

GPR survey U1 (Figure 4) consisted of 61 parallel lines with 61 stations per line. The grid size was 15 × 15 m; the line and station separations were both 25 cm. The data were recorded using two 200 MHz antennas with a constant offset of 3.0 m.

GPR survey U2 (Figure 4) consisted of 51 parallel lines with 51 stations per line. The grid size was 25×25 m; the line and station separations were both 50 cm. The data were recorded using two 100 MHz antennas with a constant offset of 3.0 m.

GPR data processing

Preliminary processing of the GPR data consisted of editing and header corrections, de-bias and time-zero corrections, filter and gain analysis, CMP velocity analysis, gain application, spherical divergence correction, trace mixing, and plotting. The surface topography was sufficiently planar that elevation statics were not applied.

Figure 5 contains two representative CMP gathers. These illustrate the overall quality of the data. There are significant lateral variations in structure, which make the corresponding velocity analyses (which assume horizontal layers), less reliable. A velocity of 0.072 m/ns, obtained from CMP velocity analysis, was used for depth conversion (3.58 m/100 ns) for all the profile plots. To facilitate geologic interpretation, the depth scales on all the GPR data plots are shifted to correspond closely with the corresponding positions in the measured section in Figure 3. Prominent reflections (labeled A and B) in Figures 5a and 5b are interpreted as originating from the unconformity at 10.7 m and the mudstone-to-sandstone contact at 21.3 m, respectively (Figure 3). A also corresponds to a large (six-fold) increase in gamma-ray count above an otherwise fairly constant background over the rest of the measured section. A high gamma ray count is usually associated with concentration of radioactive minerals by leaching and oxidation at erosional unconformities.

All GPR profiles are plotted with a 3 trace mix to reduce random noise and to enhance the continuity of the near-horizontal features. An approximate spherical divergence correction and a time-dependent gain function (that compensates for attenuation) were applied to make the deeper features more visible. The 3-D volume plots included 2-D smoothing over the visible volume faces.

Analysis of 3-D survey U1

Reconnaissance and outcrop photography indicate that units GS 6 and 7 are present at the U1 GPR site (Figures 2 and 3). The GS 7 tidal channel complex is absent over much of U1 except in the northern and eastern corners of the survey area because of recent erosion. It is probable that the coal-bearing

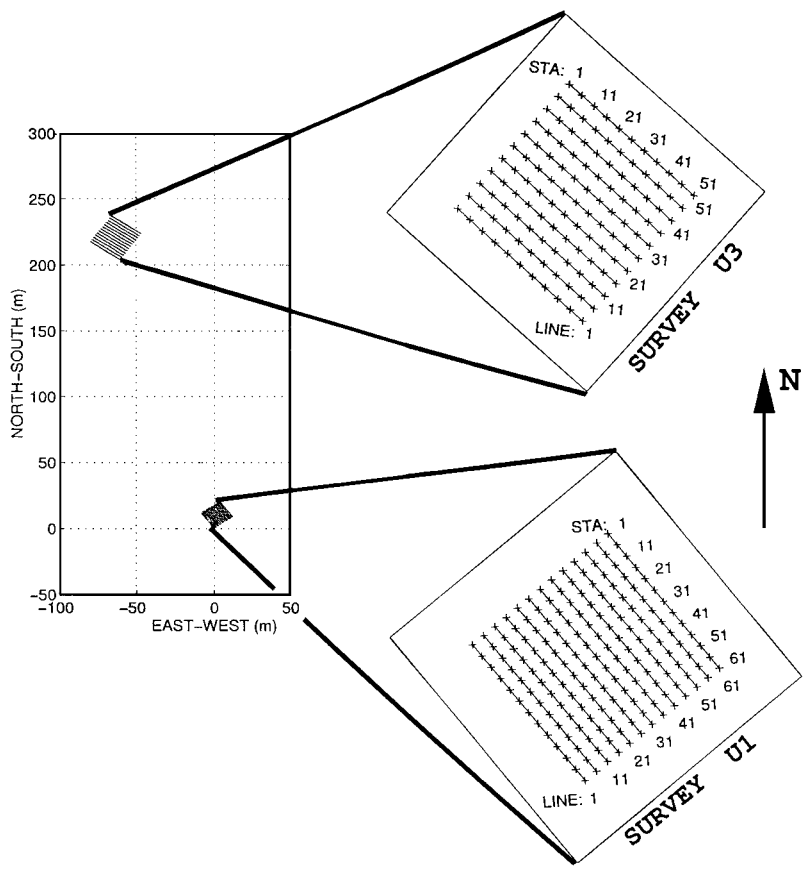

FIG. 4. 3-D survey locations. The box at the left is the same as that outlined in Figure 1b. In the following plots, GPR lines are designated by the survey name (U1 or U3) followed by the line number (for example, U1-11 is the eleventh line in survey U1). Any individual trace is designated by its station number with the line, which also corresponds to its midpoint number.

sequence is uniformly dipping throughout the survey site and so may be used as a reference reflector.

Figures 6a and 6b show representative shallow data (0 to 100 ns) from lines U1-11 and U1-21. These are the eleventh and twenty-first 2-D lines that make up the 3-D data volume. The upper 3 m of the section at the adjacent outcrop (Figure 3) contain small-scale lenticular features that are interpreted as tidally reworked deltaic lithofacies. These lenses are underlain by a silty/coal layer (1 m thick) and a fractured channel complex (4.0–14.0 m depth).

On line U1-11 (Figure 6a), prominent lenticular features (e.g., those labeled A, B, and C) between 20 and 70 ns are interpreted as bedforms associated with channel fill and shale drapes (compare with the outcrop data in Figure 3). Their thicknesses are approximately 0.25 m. The same features were identified on an average of five adjacent lines. From 70 to 80 ns is a low-amplitude zone (labeled D), probably the silty coal layer. Deeper in the section (80–90 ns) is an event (labeled E) that extends across the whole line and is probably the top of the thicker channel complex (Figure 3). Line U1-21 (Figure 6b) shows similar features. F through H are interpreted as sandstone lenses; N, the silty coal; and O, the top of the channel complex.

Figure 7 shows the complete section (0–300 ns) for line U1-52. Here, the upper tidal channel unit (labeled A) is thicker than the corresponding unit in Figure 6 since the topographic surface is stratigraphically slightly higher because of differential erosion. The reduction in coherent GPR reflections below 4 m depth is consistent with the massive character of the sandstone between 4 and 14 m (Figure 3).

One of the main benefits of doing a 3-D GPR survey is that the 3-D shape and extent of the sedimentary features can be directly imaged. For survey U1, part of the data are displayed as a 3-D volume in Figure 8. The slices shown on the cube faces were chosen to illustrate the spatial continuity of the features within and across slices. The horizontal slice on the top of the cube corresponds approximately to the center of the reworked tidal channel complex. The geometry and continuity of the sandstone lenses are clearly visible. In the outcrop, these lenses correspond to sigmoidally cross-stratified sandstone bodies with horizontal dimension about 3 m in the northeast to southwest direction, but with a clear elongation in the northwest to southeast direction.

Analysis of 3-D survey U3

The second survey grid (U3) is located within the GS 6 unit. Examination of the outcrop west of the U3 site demonstrates significant lateral continuity of both internal channel

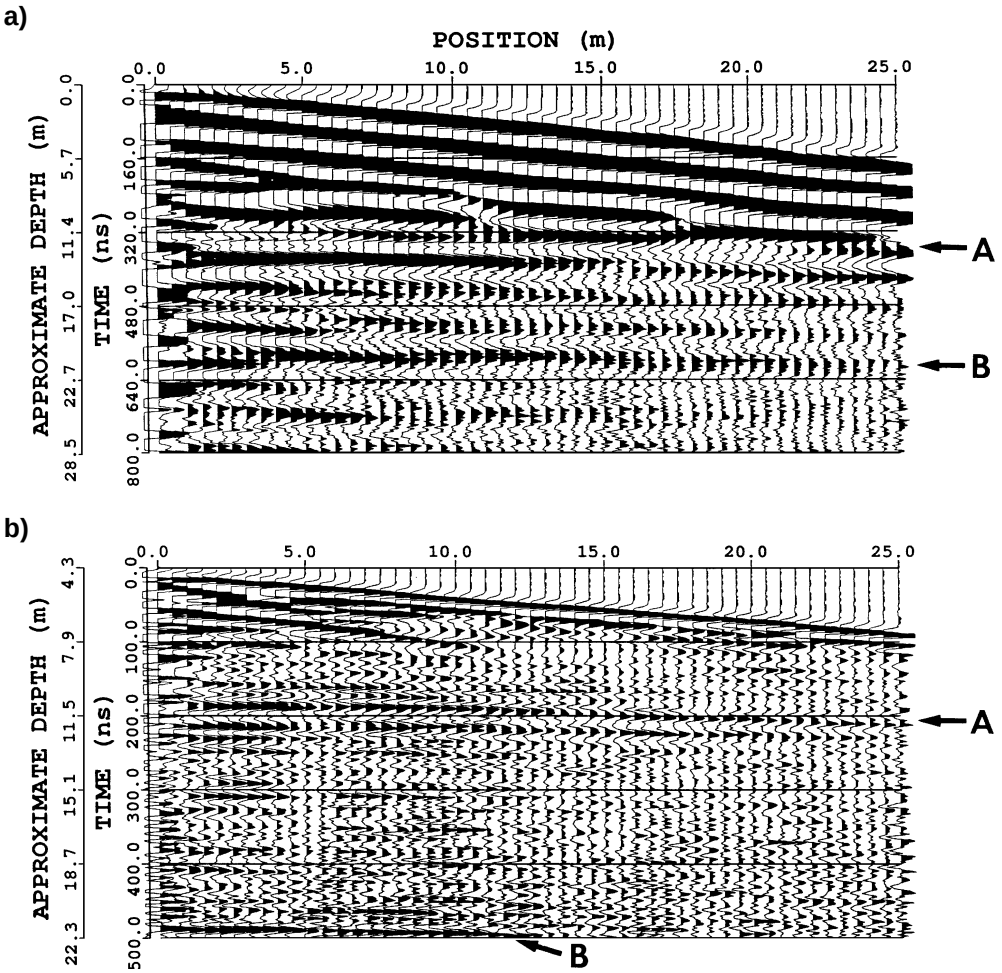

FIG. 5. Two representative CMP gathers. (a) is 50 MHz data collected along line 1 of survey U1; (b) is 100 MHz data collected along line 25 of survey U3.

boundaries, and of the underlying GS 5 coal-bearing sandstone and muddy siltstone. Minor pinch and swell and channelling are observed in the sandstones.

This survey was done at a larger station spacing than U1 because of the larger scale features seen at the outcrop. The shallow tidally reworked section and the underlying carbonaceous siltstone are missing because of recent erosion. The topographic surface here is approximately at the unconformity at 4.3 m in the measured section (Figure 3). Figure 9a shows the shallow (0–200 ns) GPR data on line U3-11. The environment here is a stacked distributary-to-nearshore sandstone lithofacies. A prominent dipping feature (between the large arrows) probably represents a large-scale channel feature since it is visible across many lines. The geometry is also consistent with this interpretation; the lower units appear to be truncated and the overlying ones exhibit downlap.

Figure 9b shows the complete section (0–550 ns) for line U3-23. This shows the expected sigmoidal features in the shallow section, bounded below by a fairly coherent reflection (labeled A) that is again interpreted as the unconformity at 10.7 m (Figure 3). A deeper coherent reflection (labeled C) can be correlated in depth with the unconformity between GS 6 and GS 5, and another (labeled B) can be correlated with the mudstone-to-sandstone contact at 21.9 m.

In the 3-D volume plot of the U3 data (Figure 10), there appears to be greater lateral continuity than there is in U1. The dominant horizontal scale in the SW to NE direction is about 8 m, but again there is significant elongation in the SE to NW direction.

DISCUSSION AND CONCLUSIONS

The feasibility of using GPR for investigation of 3-D internal structure of fluvial systems is demonstrated. The data show structures of the expected scales and spatial relationships. Correlation of the GPR data with outcrop/section data is seen on the scale of the main stratigraphic boundaries, and for the character of the internal structures (e.g., lenses and channels). Thus, it is reasonable to proceed with detailed 3-D analysis, interpretation, and visualization of the 3-D data volumes. Correlation with available petrophysical data on porosity and permeability (e.g., from in-situ minipermeameter tests), and cores, well

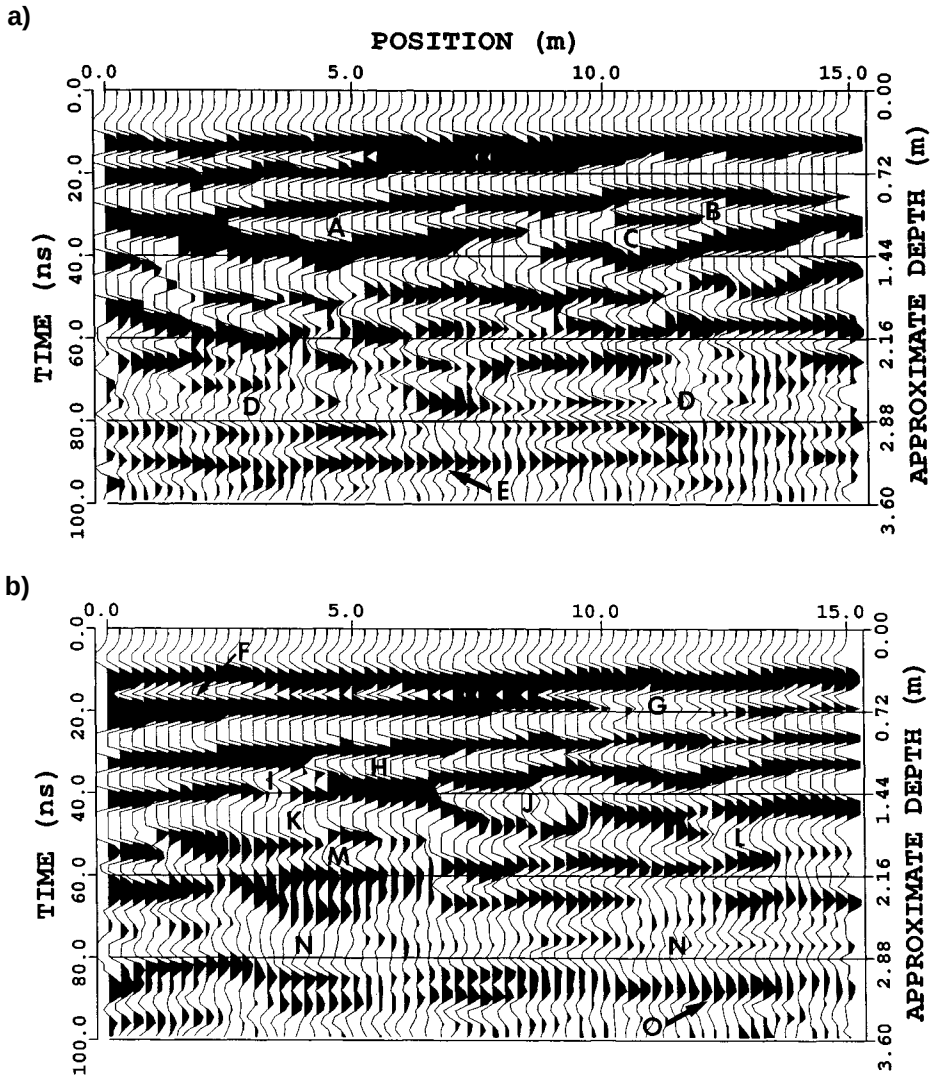

FIG. 6. Representative lines from 3-D survey U1 (line 11, above, and line 21, below). Only the first 100 ns of data are shown. Station separation is 25 cm; antenna frequency is 200 MHz. Labeled features are described in the text.

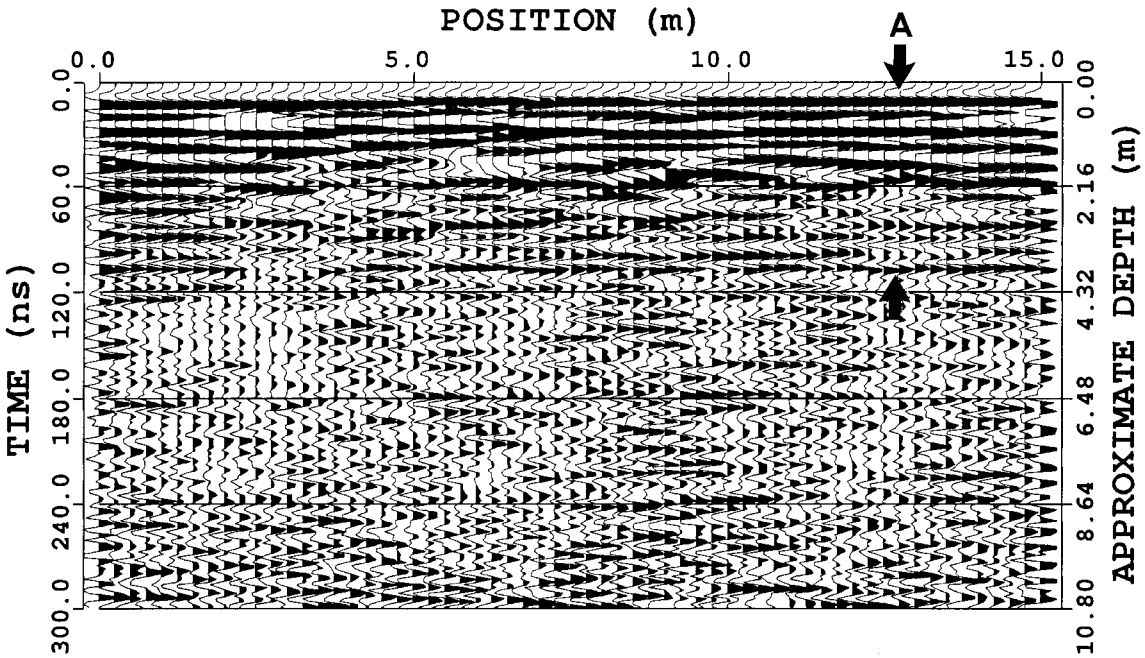

FIG. 7. Data on line 52 from survey U1. All 300 ns of data that were recorded are shown. Station separation is 25 cm; antenna frequency is 200 MHz.

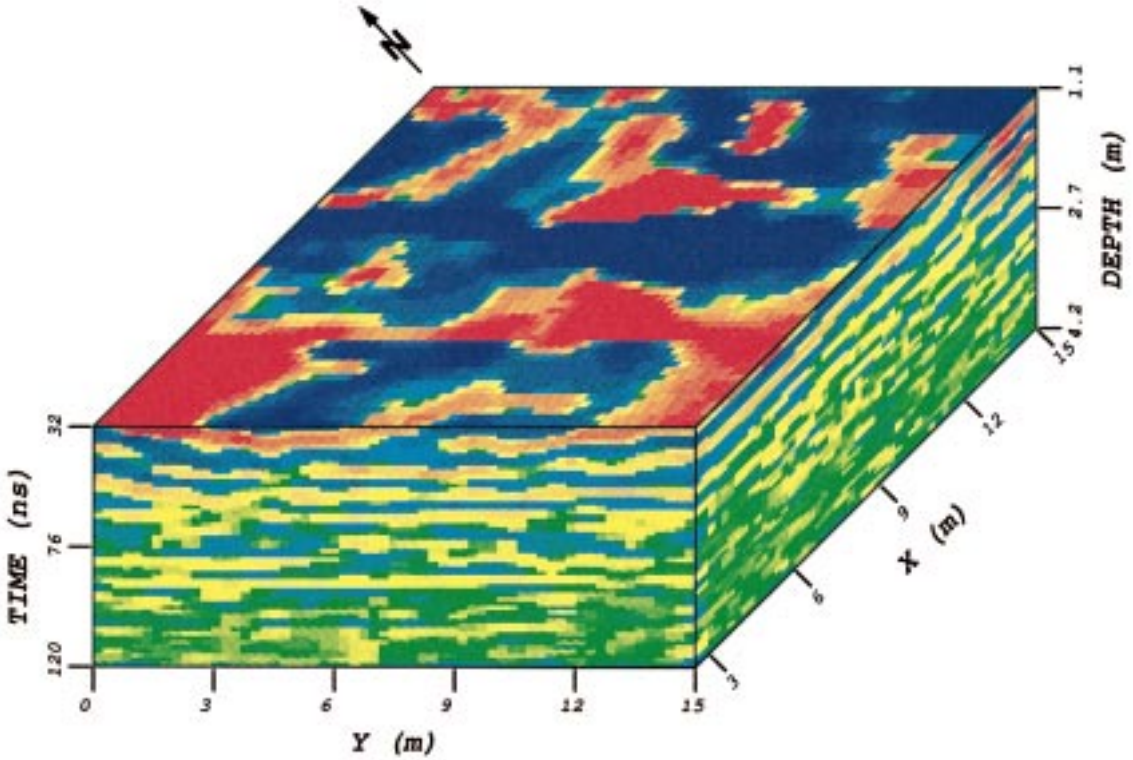

FIG. 8. 3-D perspective view of a portion of the U1 GPR data volume. The horizontal slice at the top of the volume corresponds approximately to the center of the tidally reworked zone at the top of GS 6.

logs and cuttings, and the building of reservoir models will be presented elsewhere.

The long-term goal of this research is to use the information obtained on the 3-D geometries of clastic fluvial or deltaic sandstone reservoir analogs and depositional or diagenetic reservoir barriers to construct 3-D models of subsurface reservoirs. The size of the entire surveys performed here corresponds approximately to a single model block in a typical hydrocarbon reservoir simulation. Thus, the geometrical relations and spatial distributions of properties obtained from the GPR and auxiliary measurements will need to be scaled into appropriate effective reservoir parameters at the model block scale. For other related applications, such as simulation of contaminant transport in environmental problems, the present scale may be appropriate as it is. From the geometry of the features seen in our reservoir analogs, we expect the corresponding effective fluid permeability to exhibit anisotropy.

In view of the limitations in the present data with regard to scales of stratigraphic features, it will be useful to do additional data acquisition both at finer sampling intervals and over larger areas. For example, the prominent dipping (cut and fill?) feature in Figure 9a apparently has a dimension of at least 100 m.

Finally, it would be of interest to investigate additional sites to study a greater variety of sedimentary features. It is also clear that recording in longer time windows and with lower frequencies will provide usable data to greater depths. Recording at additional antenna separations, for a least a few lines, in a 3-D survey will reduce the uncertainty in velocity estimation in such complex structures. Future studies will include direct measurements of porosity, permeability, and the electrical properties from drill cores and outcrop samples.

The successful demonstration of feasibility in this paper is a significant step toward the goal of constructing 3-D models for use both in systematic generic investigations and in simulations for specific reservoirs.

ACKNOWLEDGMENTS

The field work leading to this paper was funded by Chevron Petroleum Technology Co. Support for data analysis, software development, and publication costs was provided by the Sponsors of the UTD GPR Consortium, the NSF under grant EAR-9402386, the Texas Advanced Technology Program under grant 009741035, and the Department of Energy under grant DE-FG03-96ER14596. All GPR data were acquired with a pulseEKKO-IV GPR system, manufactured by Sensors &

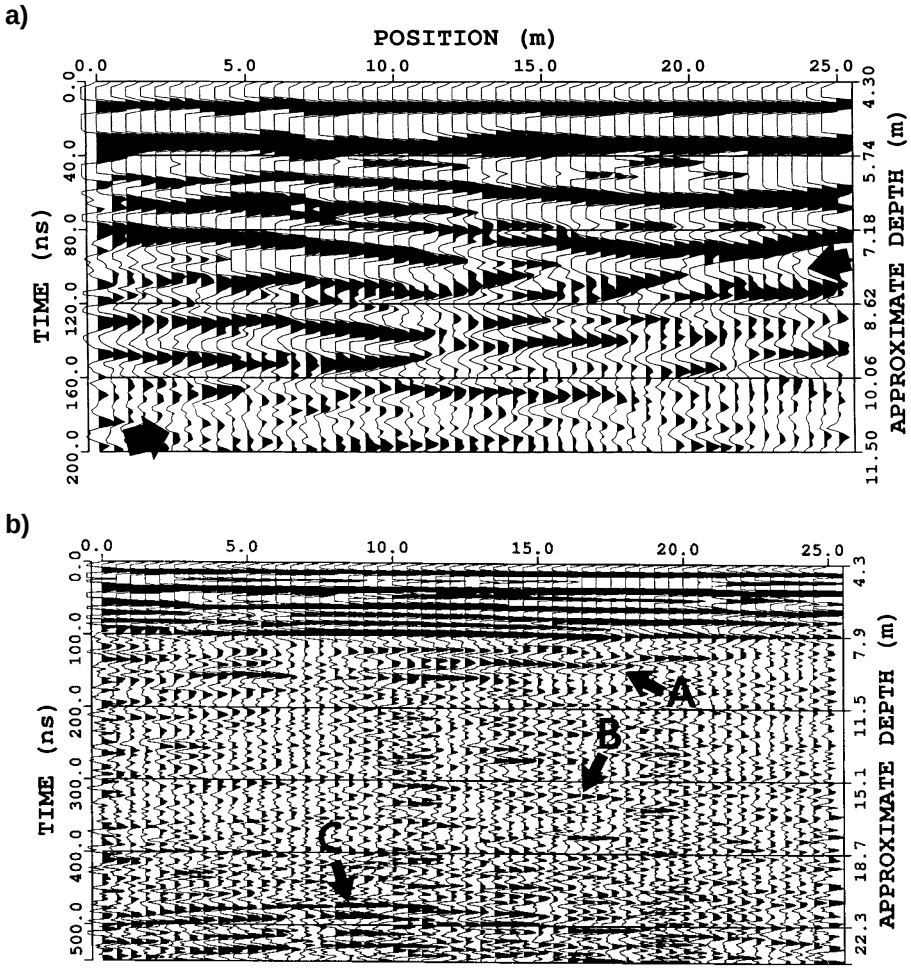

FIG. 9. (a) Line 11 from survey U3. Only the first 200 ns of data are shown. Station separation is 50 cm; antenna frequency is 100 MHz. (b) Line 51 from survey U3. All 550 ns of data that were recorded are shown. Station separation is 50 cm; antenna frequency is 100 MHz. The depth axes are shifted to correspond to the depths in Figure 3. Labeled features are described in the text.

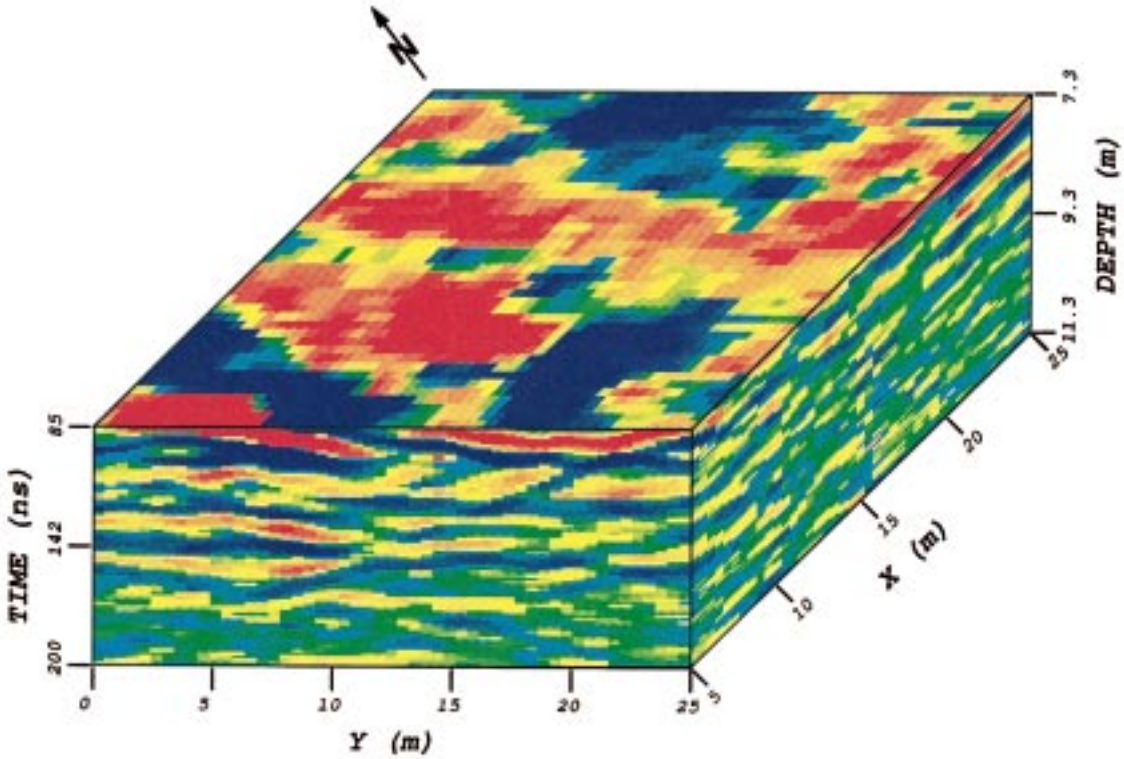

FIG. 10. 3-D perspective view of a portion of the U3 GPR data volume. The horizontal slice at the top of the volume corresponds approximately to the center of the distributary channel unit between 4.3 and 10.7 m in Figure 3. Depths are plotted to correspond with those in Figure 3.

Software, Inc., of Mississauga, Canada. The software package produced by Sensors & Software, Inc. was used for data preprocessing. The gamma-ray measurements were made using a Scintrex GIS-5 spectrometer provided by ARCO Exploration and Production. The 3-D computations were performed on a SUN-20 workstation with in-house software in the Academic Computer Center at The University of Texas at Dallas. Mr. X. Zeng assisted with the field work. This paper is contribution no. 841 from the Geosciences Department at The University of Texas at Dallas.

REFERENCES

Allen, R. L., 1979, Studies in fluvatile sedimentation: an elementary geometric model for the connectedness of avulsion-related channel sand bodies: Sed. Geol., **24**, 253–267.

Armitage, P., and Norris, R. J., 1991, An application of the "Petra" geological simulator to the Frontier Formation, Wyoming: Third Internat. Res. Charact. Tech. Conf., Tulsa, 3RC-29, 1–26.

Baker, P. L., 1991, Fluid, lithology, geometry, and permeability information from ground-penetrating radar for some petroleum industry applications: SPE-22976, Soc. Petrol. Eng., 277–286.

Boucher, R., and Galinovsky, L., 1989, RADAN 3.0: Geophysical Survey Systems Inc.

Cleavinger, H. B., 1974, Paleoenvironments of deposition of the Upper Cretaceous Ferron Sandstone near Emery, Emery County, Utah: Brigham Young Univ. Geol. Stud., **21**, 247–274.

Cotter, E., 1975, Deltaic deposits in the Upper Cretaceous Ferron Sandstone, Utah, *in* Broussard, M. L. S., Ed., Deltas, Models for Exploration: Houston Geol. Society, 471–484.

Daniels, D. J., Gunton, D. J., and Scott, H. F., 1988, Introduction to subsurface radar: IEE Proc. F, **135**, 278–320.

Davis, J. L., and Annan, A. P., 1989, Ground-penetrating radar for high-resolution mapping of soil and rock stratigraphy: Geophys. Prosp., **37**, 531–551.

Doelling, H. H., 1972, Central Utah coal fields: Sevier-Sanpete, Wasatch Plateau, Book Cliffs and Emery: Utah Geol. Mineral. Surv. Mono. Ser. 3.

Fält, L. M., Henriquez, A., Holden, L., and Tjelmeland, H., 1991, MOHERES, a program system for simulation of reservoir architecture and properties: 6th Eur. IOR Symp., 27–39.

Fisher, E., McMechan, G. A., and Annan, A. P., 1992a, Acquisition and processing of wide-aperture ground-penetrating radar data: Geophysics, **57**, 495–504.

Fisher, E., McMechan, G. A., Annan, A. P., and Cosway, S. W., 1992b, Examples of reverse-time migration of single-channel ground-penetrating radar profiles: Geophysics, **57**, 577–586.

Fisher, R. S., Barton, M. D., and Tyler, N., 1993a, Quantifying reservoir heterogeneity through outcrop characterization: 1. Architecture, lithology, and permeability distribution of a landward-stepping, fluvial-deltaic sequence, Ferron Sandstone (Cretaceous), central Utah: Gas Res. Inst. Topical Rep. GRI-93-0022.

———1993b, Quantifying reservoir heterogeneity through outcrop characterization: 2. Architecture, lithology, and permeability distribution of a seaward-stepping, fluvial-deltaic sequence, Ferron Sandstone (Cretaceous), central Utah: Gas Res. Inst. Topical Rep. GRI-93-0023.

Fisher, R. S., Tyler, N., and Barton, M. D., 1992, Quantification of flow unit and bounding element properties and geometries, Ferron Sandstone, Utah: Implications for heterogeneity in Gulf Coast Tertiary deltaic reservoirs, *in* Characterization of Reservoir Heterogeneity: Bur. Econ. Geol., UT-Austin, Austin, TX, DOE Rep. DOE/BC/14403-3, 134–168.

Gawthorpe, R. L., Collier, R. E. L., Alexander, J., Bridge, J. S., and Leeder, M. R., 1993, Ground penetrating radar: application to sand body geometry and heterogeneity studies, *in* North, C. P., and Prosser, D. J., Eds, Characterization of Fluvial and Aeolian Reservoirs: Spec. Publ. 73, Geol. Soc. London, 421–432.

Gundesö, R., and Egeland, O., 1990, SESIMIRA—a new geological tool for 3-D modeling of heterogeneous reservoirs, *in* Buller, A. T., Berg, E., Hjelmeland, O., Kleppe, J., Torsoeter, O., and Aasen, J. O., Eds, North Sea Oil and Gas Reservoirs—II: Proc. 2nd North Sea Oil and Gas Reservoirs Conf., 363–371.

Haldorsen, H. H., and Damsleth, E., 1990, Stochastic modeling: J. Petr. Tech., 404–412.

Hale, L. A., 1972, Depositional history of the Ferron Formation, central Utah, in Plateau-Basin and Range Transition Zone: Utah Geol. Assoc., 29–40.

Henriquez, A., Tyler, K. J., and Hurst, A., 1990, Characterization of fluvial sedimentology for reservoir simulation modeling: Soc. Petr. Eng. Form. Eval., **5**, 211–216.

Jordan, D. W., and Pryor, W. A., 1992, Hierarchial levels of heterogeneity in a Mississippi River meander belt and application to reservoir systems: Am. Assn. Petr. Geol. Bull., **76**, 1601–1624.

Katich, P. J., Jr., 1954, The startigraphy and paleontology of the pre-Niobrara Upper Cretaceous rocks of Castle Valley, Utah: M.S. thesis, Ohio State Univ., Columbus.

Lowry, P., 1990, Facies architecture of delta front reservoirs: Implications for reservoir characterization: Rep. no. IKE/KR/ F-90/129, Inst. Energiteknikk, Kjeller, Norway.

Mayer, D. F., and Chapin, M. A., 1991, A comparison of outcrop and subsurface geologic characteristics in the Cretaceous J Sandstone: Third Internat. Res. Charact. Tech. Conf., Tulsa, 3RC-29, 1–26.

Meyers, R. A., Smith, D. G., and Jol, H. M., 1994, Ground penetrating radar investigation of the internal structure of a Pacific coast barrier spit: Abstr. with Prog., Geol. Soc. Am., **26**, 69.

Miall, A. D., 1988, Reservoir heterogeneities in fluvial sandstones: lessons from outcrop studies: Am. Assn. Petr. Geol. Bull., **72**, 682–697.

Polasek, T. L., and Hutchinson, C. A., 1967, Characterization of non-uniformities within a sandstone reservoir from a fluid mechanics standpoint: Proc., 7th World Petr. Cong., Mexico City, 397–407.

Pratt, B. R., and Miall, A. D., 1993, Anatomy of a bioclastic grainstone megashoal (Middle Silurian, southern Ontario) revealed by ground-penetrating radar: Geology, **21**, 223–226.

Ravenne, C., Eschard, R., Galli, A., Mathieu, Y., Montadert, L., and Rudkicz, J-L., 1987, Heterogeneities and geometry of sedimentary bodies in a fluvio-deltaic reservoir: SPE-16752, Soc. Petr. Eng., 115–122.

Ryer, T. A., 1981a, Delatic coals of the Ferron Sandstone Member of the Mancos Shale: predictive model for Cretaceous coal-bearing strata of the Western Interior: Bull. Geol. Assn. Am., **65**, 2323–2340.

——— 1981b, The Muddy and Quitchupah projects: a project report with descriptions of cores of the I, J, and C coal beds from the Emery coal field, central Utah: U.S. Geol. Surv. open-file rep. 81–460.

——— 1983, Transgressive-regressive cycles and the occurrence of coal in some Upper Cretaceous strata of Utah: Geology, **111**, 207–210.

Ryer, T. A., and McPhillips, M., 1983, Early Late Cretaceous paleogeography of east-central Utah, *in* Reynolds, M. W., and Dolly, E. D., Eds., Mesozoic Paleogeography of the West-central United States: Rocky Mountain Section, Proc., Soc. Econ. Paleont. Mineral. Symp., **2**, 253–272.

Ryer, T. A., Phillips, R. E., Bohor, B. R., and Pollastro, R. M., 1980, Use of altered volcanic ash falls in stratigraphic studies of coal-bearing sequences: an example from Upper Cretaceous Ferron Sandstone Member of the Mancos Shale in central Utah: Geol. Soc. Am. Bull., **91**, 579–586.

Stalkup, F. I., and Ebanks, W. J., Jr., 1986, Permeability variation in a sandstone barrier island-tidal channel-tidal delta complex, Ferron Sandstone (Lower Cretaceous), central Utah: SPE-15532, Soc. Petrol. Eng., 1–8.

Thompson, S. L., 1985, Ferron Sandstone member of the Mancos Shale: a Turonian mixed-energy deltaic system: M.A. thesis, Univ. of Texas, Austin.

Tomutsa, L., Chang, M-M., and Jackson, S., 1991, Application of outcrop data for characterizing reservoirs and deriving grid-block scale values for numerical simulation: Third Internat. Res. Charact. Tech. Conf., Tulsa, 3RC-08, 1–18.

Tyler, N., Barton, M. D., Bebout, D. G., Fisher, R. S., Grigsby, J. D., Guevara, E., Holtz, M., Kerans, C., Nance, H. S., and Levey, R. A., 1992, Characterization of oil and gas reservoir heterogeneity: DOE rep. 14403-3.

Uresk, J., 1979, Sedimentary environment of the Cretaceous Ferron Sandstone near Caineville, Utah: Brigham Young Univ. Geol. Stud., **26**, 81–100.

Weber, K. J., and van Geuns, L. C., 1989, Framework for constructing clastic petroleum simulation models: SPE-19582, Soc. Petrol. Eng., 109–118.

Wright, D. L., Bradley, J. A., and Hodge, S. M., 1989, Use of a new high-speed digital acquisition system in airborne ice-sounding: IEEE Trans. Geos. Rem. Sens., **27**, 561–567.